

## PHOSPHATING OF CARBON STEEL IN CONCENTRATES, CONTAINING IN VARIOUS RATIOS ZINC AND MANGANESE PHOSPHATES

Phosphating, originally intended mainly to protect metals from corrosion using relatively thick layers, is known to be one of the most important and widely used forms of metal surface pretreatment. Its range of applications nowadays has expanded considerably, including as solid lubricants in wire drawing, calibration and cold forming of metals, for electrical insulating coatings, as a sublayer prior to the application of varnish and polymer coatings, etc. The results obtained when phosphating low carbon steel in phosphate concentrates with different ratios of the zinc and manganese phosphates, contained therein, are presented in the proposed work. The main parameters characterizing the phosphate concentrates – density, pH, electrical conductivity, total and free acidity have been determined. The influence of temperature and concentration of phosphating solutions on the mass/thickness of the coatings and on the dissolved metal of the substrate, depending on the duration of the phosphating process, was investigated. The structure, elemental and phase composition of the phosphate coatings obtained have been determined by various physical – analytical methods.

*Keywords:* Phosphating; conversion coatings; steel surfaces; corrosion

### 1. Introduction

The phosphating of metals and especially Fe-C alloys is among the most important and employed worldwide processes of preliminary metal treatment. The area of application of phosphating, conceived as a corrosion protector, has been developed in the past decades [1-3]. This concerns their applications as sublayers in: the painting processes, the polymeric coatings as well as surfactants under the deep metal drawing processes [4-7]. The increase of the energy cost needs a development of low-temperature phosphating keeping the properties of the coatings [8-16]. This paper presents the results obtained under phosphating of mild steel surfaces in water solutions of concentrates containing zinc and manganese phosphates in different ratios.

purchased material (see TABLE 1). The preparation of the testing samples includes sequentially: degreasing in an alkaline degreaser, washing with cold water, pickling in 15% HCl solution + inhibitor and rinsing with running water.

The electrochemical experiments were carried out with plate-shaped specimens with a fixed working surface area of  $1 \times 10^{-3} \text{ m}^2$ . In addition, samples with a form of a disk ( $1 \times 10^{-4} \text{ m}^2$ ) were used as specimens for the physical – analytical methods applied in the study.

TABLE 1

Chemical composition of the steel (% in mass)

C	Mn	Si	P	S	Cr	Ni	Cu
0.17	0.36	0.016	0.01	0.029	0.06	0.06	0.11

### 2. Experiment

#### 2.1. Material and samples

In the present article, prepared square samples (thickness 1.0 mm and working surface  $5 \times 10^{-3} \text{ m}^2$ ) were investigated. The chemical composition is taken from the certificate of the

#### 2.2. Solutions

The phosphating liquid concentrate contains zinc and manganese orthophosphates, phosphoric acid, inorganic activators, stabilizing agents as well as surfactants are added. The zinc phosphates contained in phosphating concentrates are as follows: 90, 70, 50, and 30%.

<sup>1</sup> UNIVERSITY OF CHEMICAL TECHNOLOGY AND METALLURGY, FACULTY OF CHEMICAL TECHNOLOGY, 8 KLIMENT OHRIDSKI BLVD., 1756 SOFIA, BULGARIA

\* Corresponding author: [dimkaivanova@uctm.edu](mailto:dimkaivanova@uctm.edu)



The working media are aqueous solutions of the phosphating preparation with concentrations in the range of 5.0-20.0 vol.%. The experiments are carried out in a temperature range 60-90°C and a process duration 0.5-20.0 min. The working/model media used for the corrosion experiments is 0.6 M NaCl.

## 2.3. Methods

### 2.3.1. Gravimetric method

The gravimetric method was used to study the kinetics of forming and determining the process conditions for the phosphate coating's mass/thickness growth, depending on the effect of different factors. The method allows determining a mass/thickness alteration after forming and removing the coatings:

$$M_1 = \frac{m_2 - m_3}{S}, \text{ g m}^{-2} \quad (1)$$

$$M_2 = \frac{m_1 - m_3}{S}, \text{ g m}^{-2} \quad (2)$$

$$M_3 = \frac{m_2 - m_1}{S}, \text{ g m}^{-2} \quad (3)$$

where:  $M_1$ ,  $\text{g m}^{-2}$  is the mass (or accepted to call a thickness) of the obtained coating (1);  $M_2$  dissolved mass of metal substrate (2);  $M_3$  – alteration of the sample mass under phosphating (3);  $m_1$ ,  $m_2$  and  $m_3$  are respectively the sample mass before and after forming of the coating, and after removal of the coating,  $S$  – sample surface area,  $\text{m}^2$ .

### 2.3.2. Electrochemical methods

Electrochemical measurements were performed in a three-electrochemical cell, which combines a galvanic cell between the working and reference electrodes and an electrolysis cell, between the working and counter electrodes.

*Open circuit potential determination.* The corrosion potentials are not indicative with respect to the resistance attained but their values and time variations provide enough information about the character of the corrosion process, the behavior of both the metal and metal coating in different media under various conditions. The experiments were performed with an automatic device EG&G Princeton Applied Research, Potentiostat/Galvanostat, Model 263A. All electrochemical measurements were performed in a model 0.6 M NaCl solution.

### 2.3.3. Physical methods

*Scanning electron microscopy (SEM).* The morphology and structure of the coatings were examined by scanning electron microscopy, using a SEM/FIB LYRA I XMU, TESCAN electron microscope, equipped with ultrahigh-resolution scanning system secondary electron image (SEI).

*Atomic emission spectral analysis (ICP).* Inductively coupled plasma (ICP) is widely used for the analysis of basic and impurity elements in various mineral raw materials and geological objects. The analysis was carried out on a Varian Vista MPX device.

*X-ray structural method (XRD).* A PANalytical Aeris diffractometer with  $\text{CuK}\alpha$  radiation (40 kV, 15 mA), wavelength  $\lambda = 1.5406 \text{ \AA}$  and  $\theta$ - $\theta$  Bragg-Brentano geometry was used to determine the phase composition. The original radiographs were taken at room temperature, constant scanning speed and reflection angle  $2\theta$  in the interval  $5$ - $90^\circ$  with a step of  $0.02^\circ$ , 60 s. The resulting diffractograms were interpreted using the PDF 2-2022 database, ICDD.

## 2.4. Results and Discussion

TABLE 2 presents the values of the most important indicators characterizing these concentrates: density,  $\rho$ ; pH; conductivity,  $\sigma$ ; total,  $K_{ta}$  and free,  $K_{fa}$  acidity.

TABLE 2

Indicators of phosphating preparations

No	Phosphate solutions	$\rho$ , $\text{g/cm}^3$	pH	$\sigma$ , $\text{mS/cm}$	$K_{ta}$	$K_{fa}$
1	90 Zn	1.34	0.39	188.9	376	67
2	70 Zn	1.323	0.37	182.0	357	77
3	50 Zn	1.32	0.25	183.1	342	85
4	30 Zn	1.312	0.17	184.6	340	90

From the data in TABLE 2, it follows that as the content of manganese phosphate in the concentrate increases, its density decreases (albeit slightly), the pH decreases more than twice at its highest amount, and its conductivity remains relatively constant. Total acidity decreases, and free acidity increases. All these results can be explained by the difference in the properties of zinc and manganese phosphates contained in the concentrates in different ratios.

### 2.4.1. Gravimetric measurements

During the gravimetric studies, the influence of the parameters of the solutions (concentration and temperature) and the duration of the phosphating process on the thickness of the deposited coating –  $M_1$ , the amount of dissolved metal on the substrate –  $M_2$  and the change in the mass of the samples –  $M_3$  during phosphating was determined.

The optimal phosphating conditions (concentration of working solutions 15 vol.% and temperature range 60-90°C) have been determined experimentally, and the criteria for their selection are the preparation of a dense, uniform phosphate film on the surface of the samples and the stability of the working solutions.

Fig. 1 shows typical relationships "thickness of phosphate coatings – time" obtained at different temperatures of the phos-

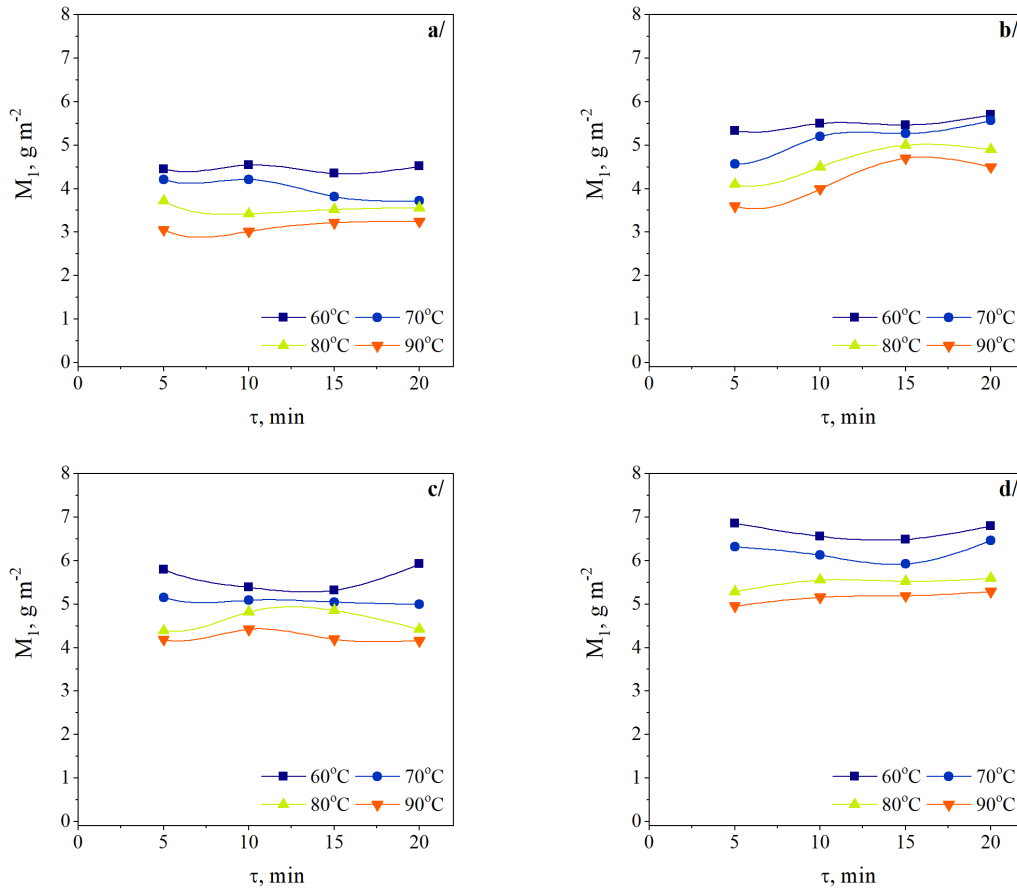


Fig. 1. Influence of the phosphating time,  $\tau$ , on the thickness of the resulting phosphate coatings: a/ 30 Zn; b/ 50 Zn; c/ 70 Zn; d/ 90 Zn

phating solutions (15 vol.%). From the course of the curves, it can be seen that the thickness of the formed coatings is maximum after about 5-7 minutes from the beginning of the process, and this time rises with increasing content of manganese phosphates in the solution. A gradual reduction in  $M_1$  values followed, most likely due to the reorganization and compaction of the coatings.

Fig. 1 also shows that the thickest coatings, for all investigated temperatures, are obtained in the solutions with the highest content of zinc phosphate – 90 Zn, and with its decrease (resp. increase of manganese phosphate in the solution) the coatings become gradually thinner. In addition, increasing the content of manganese phosphates leads to a change in the influence of temperature on the thickness of the formed films. While at 90 Zn (with the lowest content of manganese phosphate) the values of  $M_1$  increase with increasing of temperature, this influence is reversed for the other phosphating preparations.

All these regularities can be related to the different influence of the two phosphates on the genesis and growth rates of phosphate crystals in the studied temperature interval.

Fig. 2 illustrates the change in the mass of the dissolved metal of the substrate,  $M_2$  in the process of obtaining phosphate coatings. As should be expected from the mechanism of the phosphating process itself, this mass increases with time and the temperature of the working solutions. The dependencies in Fig. 2 also show that the increase of manganese phosphates in

the solutions leads to an increase in  $M_2$  values, which can be related both to the decrease in pH under these conditions and to the known difficulties of nucleation in manganese compared to zinc phosphating.

The change in the mass of the test samples during their phosphating,  $M_3$  is shown in Fig. 3. It follows from the course of the curves that, apart from phosphating in 90 Zn (Fig. 3), where up to about 10 minutes the mass of the obtained coating is greater than the mass of the dissolved metal on the substrate, in the other phosphating preparations at all temperatures and concentrations, the opposite is observed – more is the dissolved metal. The amount of the latter increases with raising of temperature and the content of manganese phosphates in the solutions.

Since the preparations studied in the article were designed as high-speed (the ratio  $P_2O_5 : NO_3^{-1} = 1:3$ ), it was interesting to understand how the phosphating processes proceed in their initial period of up to 5 minutes. In Fig. 4 shows the changes in the values of  $M_1$ ,  $M_2$  and  $M_3$  obtained at the same concentration and temperature of the different phosphating preparations. From Fig. 4a/, it follows that the phosphate coatings are formed relatively quickly, and this tendency definitely decreases when the content of manganese phosphates in the solutions increases – from 90 Zn to 30 Zn. In the same way, the thickness of the coatings is also changed.

The curves  $M_2 - \tau$  (Fig. 4b/) show the exact opposite trend of the above – the mass of the dissolved metal increases with a de-

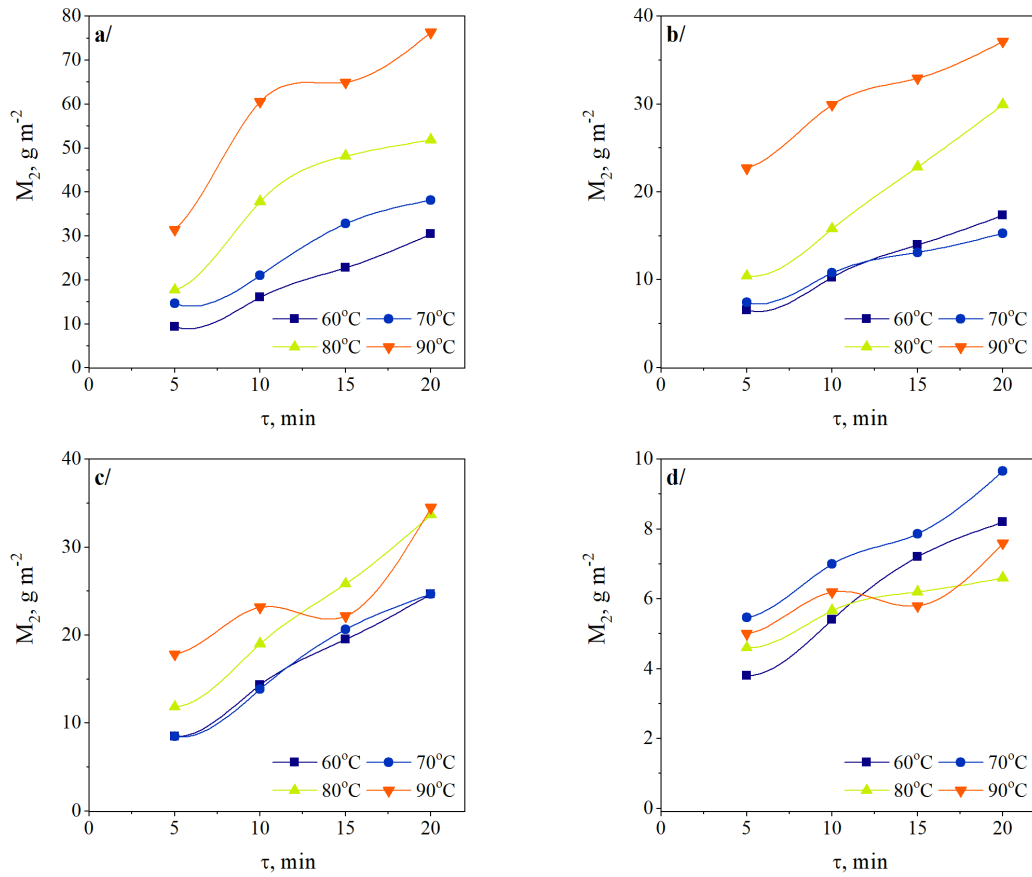


Fig. 2. Change in the mass of dissolved metal on the substrate during phosphating,  $M_2$ : a/ 30 Zn; b/ 50 Zn; c/ 70 Zn; d/ 90 Zn

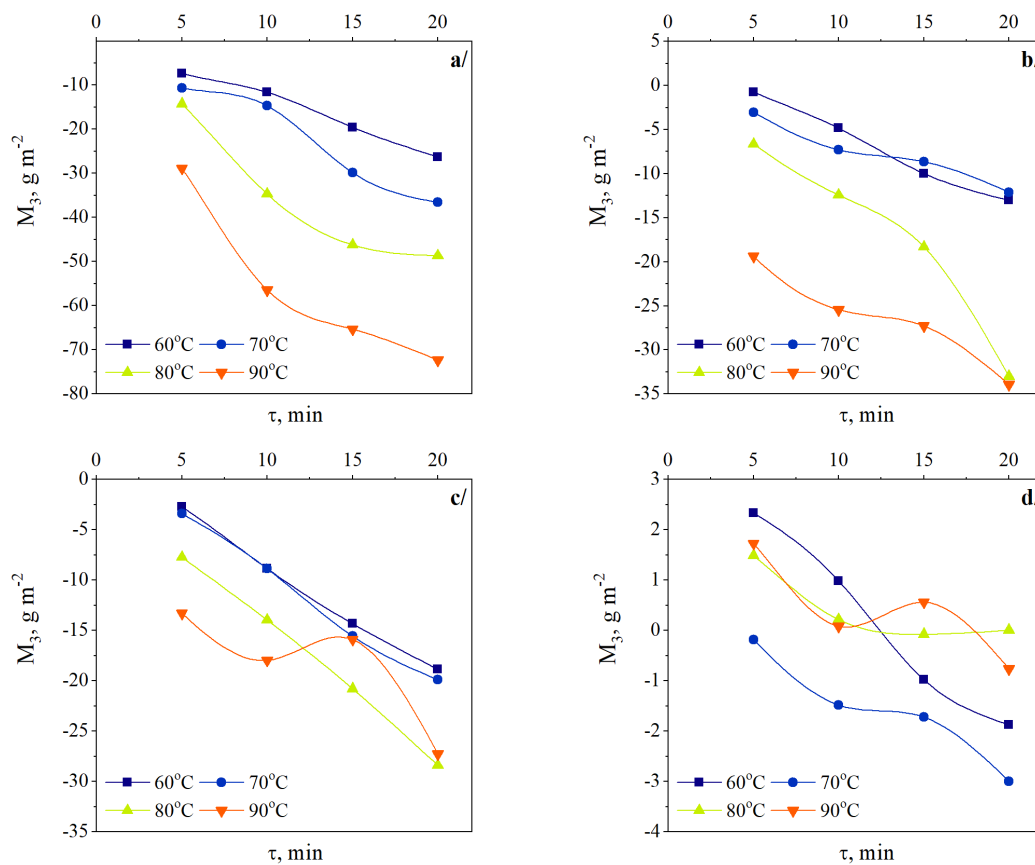


Fig. 3. Change in the mass of the experimental samples in the process of their phosphating  $M_3$ : a/ 30 Zn; b/ 50 Zn; c/ 70 Zn; d/ 90 Zn

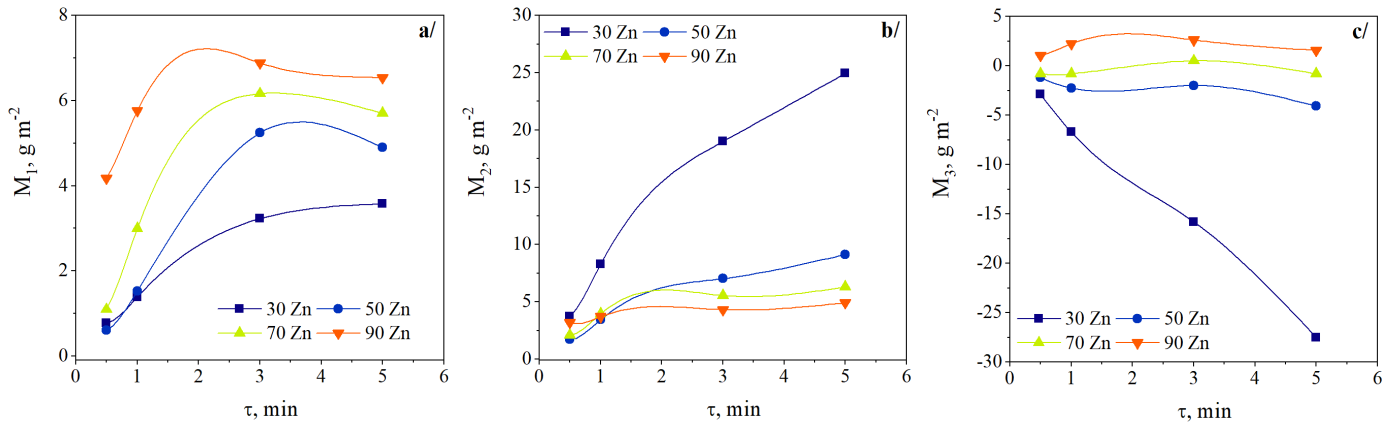


Fig. 4. Phosphating in solutions with concentrations of 15 vol.% and temperature 70°C: a/  $M_1$ ; b/  $M_2$ ; c/  $M_3$

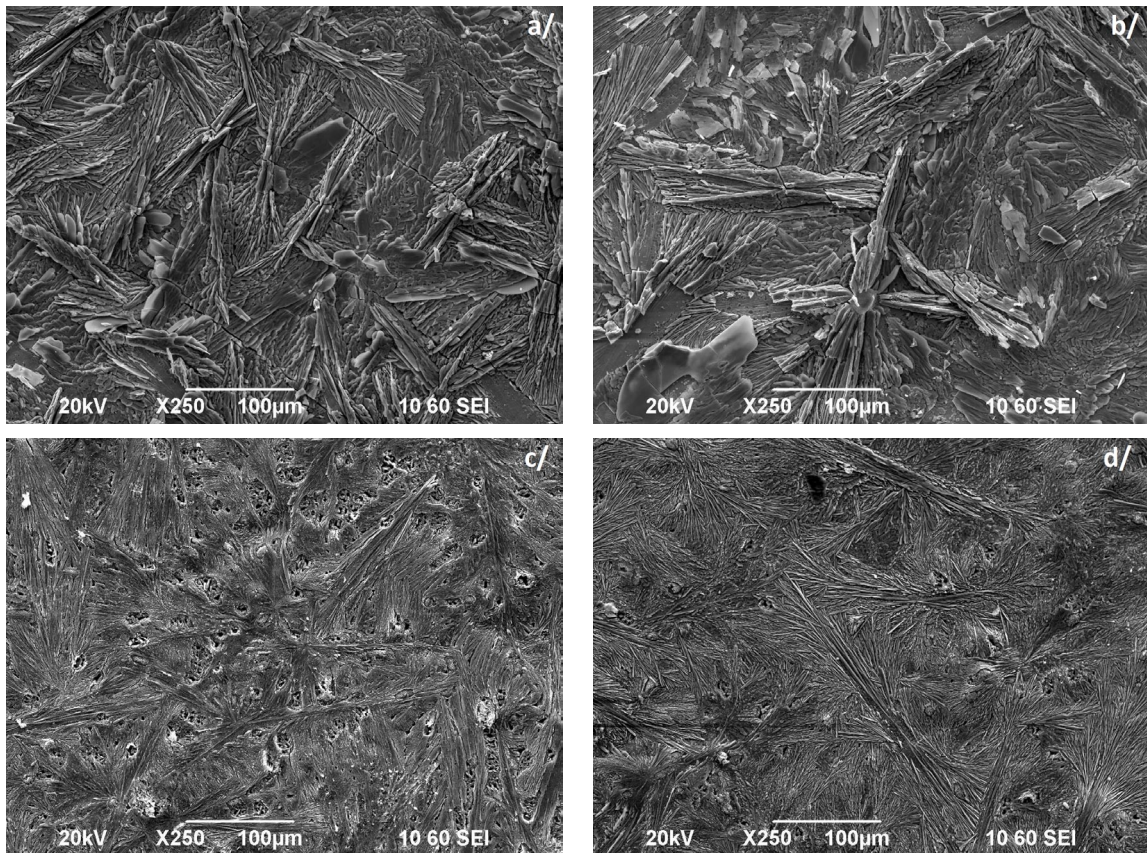


Fig. 5. SEM micrographs of the phosphate coatings obtained on mild steel samples in: a/ 30 Zn; b/ 50 Zn; c/ 70 Zn; d/ 90 Zn

crease in the content of zinc phosphate in the medium. Fig. 4c/, proves that, except for 90 Zn, during phosphating in the others, more metal is dissolved than the mass of the phosphate coating.

#### 2.4.2. SEM analysis

Fig. 5 shows micrographs (SEM) of phosphate coatings obtained on carbon steel samples in solutions of the preparations 30 Zn, 50 Zn, 70 Zn and 90 Zn, with a concentration of 15 vol.%, for a time of 10 min and a temperature of 70°C (for 30 Zn – 90°C).

It follows from the figure that the habit of the coatings is constant – the crystals are formed from a single center and grow spherulite-like. The change in the size of the crystals is visible, which decrease and become denser when the content of manganese phosphates increases.

#### 2.4.3. Atomic emission spectral analysis

The content of manganese and zinc in the coatings, determined according to the methodology described in section Methods, is shown in TABLE 3.

TABLE 3

Manganese and zinc content into the phosphate coatings

Indicators	Measure	30 Zn	50 Zn	70 Zn	90 Zn
Manganese	%	1.80	1.33	0.96	0.90
Zinc	%	6.58	8.23	9.28	25.70

The data in the table show that the changes in the amounts of manganese and zinc in the coatings follow an analogous course to the content of their phosphates in the solutions of the respective preparations. For example, the amount of zinc decreases about 4 times from 90 Zn to 30 Zn, while conversely, manganese increases twice.

#### 2.4.4. X-Ray Diffraction (XRD)

X-ray diffraction (phase) analysis was performed according to the methodology described in section Methods of the paper. The results of the XRD analysis are presented in Fig. 6.

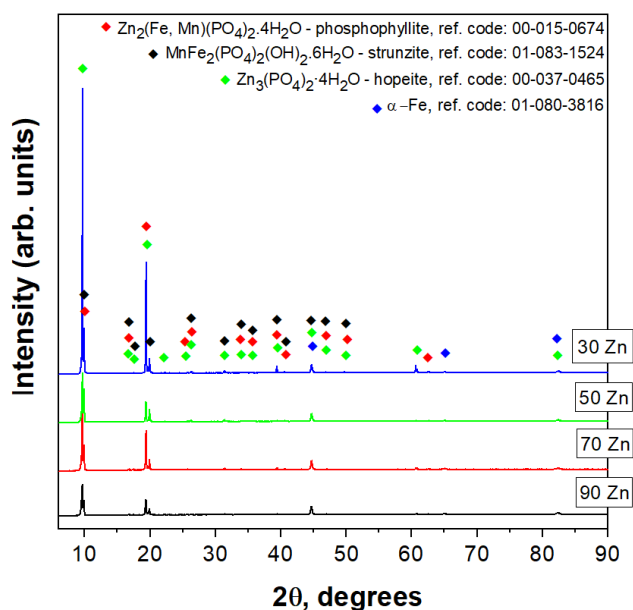


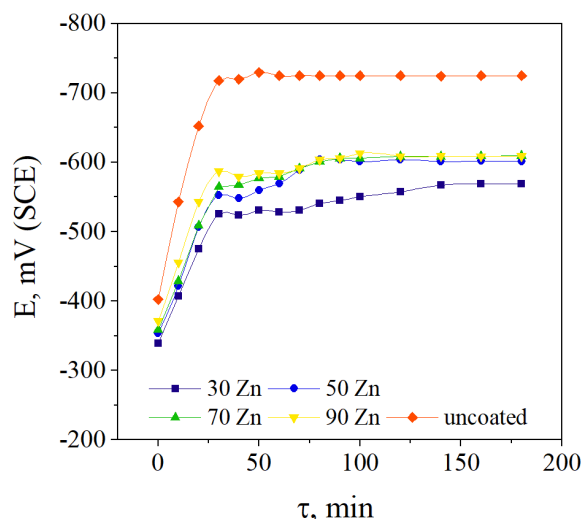
Fig. 6. XRD-spectra of the crystalline phosphate coatings

The ratio of the quantities of the phase's changes for the different phosphating solutions: in 90 Zn, hopeite predominates, followed by phosphophyllite, in which a partial replacement of iron with manganese is found –  $Zn_2(Fe, Mn)(PO_4)_2 \cdot 4H_2O$ . As the content of manganese phosphates increases, the amount of hopeite decreases at the expense of phosphophyllite, and in 50 Zn and especially in 30 Zn, strunzite and mixtures of them are formed.

#### 2.4.5. Open circuit potential determination

The corrosion resistance, resp. the protective ability of phosphate coatings is determined in 0.6M NaCl. The test itself

consists in immersing the phosphated samples in the NaCl solution. The coating is defined as stable if no changes to the surface or discoloration of the solution occur within 2 hours. Simultaneously with this test, the corrosion potential of the samples was measured (Fig. 7), and for comparison the change in the potential of a non-phosphated sample is also shown.

Fig. 7. Relationships  $E-t$ , 3.5% NaCl

It can be seen from the figure that as the content of manganese phosphates increases, the corrosion potential becomes more positive, which is evidence of the higher resistance of the coatings obtained in these solutions. After 60 min, the potentials of the coatings obtained in 90 Zn, 70 Zn and 50 Zn merge and remain constant – about 600 mV (SCE), while the corrosion potential for the one obtained in 30 Zn is about 50 mV more positive for the entire interval.

After more than 3 hours, no surface changes of the phosphated samples or coloring of the test solution (0.6M NaCl) were detected.

### 3. Conclusions

From the results obtained in the phosphating of carbon steels containing zinc and manganese phosphates in different ratios, the following conclusions can be made:

1. As the amount of manganese phosphates in phosphating preparations increases, their density, pH and total acidity decrease, free acidity increases, and their conductivity remains relatively constant.
2. As the content of manganese phosphates in the phosphating solutions increases, the mass (thickness) of the resulting coatings decreases at all investigated temperatures, and the amount of dissolved metal on the substrate increases.
3. It was established that in the investigated preparations phosphate coatings are formed in a relatively short time (3-5 min), and with increasing manganese phosphates in the solution it increases.

4. Phosphate coatings mainly consist of three phases: hopeite, phosphophyllite and strunzite, and their content varies depending on the content of zinc and manganese phosphates in the phosphating solutions.
5. Electron microscopy has shown that the habit of the phosphate coatings is preserved, with crystal sizes decreasing as the manganese phosphate content of the phosphating solutions increases.
6. It has been proven that the amount of manganese in phosphate coatings increases as the content of manganese phosphates in the phosphating solutions increases.
7. Phosphate coatings are highly resistant in 3.5% NaCl, with the corrosion potential shifting in a positive direction with increasing manganese phosphates in the phosphating solutions.

#### REFERENCE

- [1] Universal Metal finishing guidebook, Published by Metal finishing magazine, 2012-2013.
- [2] T.S.N. Sankara Narayanan, Surface Pretreatment by Phosphate Conversion Coatings – A Review. *Rev. Adv. Mater. Sci.* **9**, 130-177 (2005).
- [3] J. Donofrio, Zinc Phosphating, *Metal Finishing* **98**, 57-73 (2000).
- [4] N. Rezaee, M.M. Attar, B. Ramezanzadeh, Studying corrosion performance, microstructure and adhesion properties of a room temperature zinc phosphate conversion coating containing Mn<sup>2+</sup> on mild steel. *Surf. Coat. Technol.* **236**, 361-367 (2013). DOI: <https://doi.org/10.1016/j.surfcoat.2013.10.014>
- [5] V.I. Ivanova, Y. Trifonova, P. Petkov, Stress investigation in Ge-Te-In thin films. *Journal of Optoelectronics and Advanced Materials* **22** (5-6), 266-271(2020).
- [6] L.C. Deepa, S. Satiyanarayanan, C. Marikkannu, D. Mukherjee, Effect of divalent cations in low zinc ambient temperature phosphating bath. *Anti-Corrosion Methods and Materials* **50** (4), 286-290 (2003).
- [7] M. Tamilselvi, R. Kamaraj, M. Arthanareeswari, S. Devikala, J. Arockia Selvi, Progress in Zinc Phosphate Conversion Coatings: A Review. *IJACSA* **3**. 1 (2015).
- [8] D. Zimmermann, A.G. Munoz, J.W. Schultze, Formation of Zn-Ni alloys in the phosphating of Zn layers. *Surf. Coat. Technol.* **197** (2-3), 260-269 (2005). DOI: <https://doi.org/10.1016/j.surfcoat.2004.07.129>
- [9] H. Alizadeha, and al., Effect of Ca<sup>2+</sup> additives on morphology, composition and corrosion resistant of Zn–12%Ni phosphate coating. *J. Mater. Res. Technol.* **5** (4), 327-332 (2016). DOI: <https://doi.org/10.1016/j.jmrt.2016.03.003>
- [10] D. Ivanova, Phosphating of mild steel in zinc-manganese-nickel phosphates in different correlations. *Journal of Chemical Technology and Metallurgy* **54** (5), 1072-1078 (2019).
- [11] E.P. Banczek, P.R.P. Rodrigues, I. Kosta, The effects of niobium and nickel on the corrosion resistance of the zinc phosphate layers. *Surf. Coat. Technol.* **202** (10), 2008-2014 (2008). DOI: <https://doi.org/10.1016/j.surfcoat.2007.08.039>
- [12] M.M. Jalili, S. Moradian, D. Hosseinpour, The use of inorganic conversion coatings to enhance the corrosion resistance of reinforcement and the bond strength at the rebar/concrete. *Construction and Building Materials* **23** (1), 233-238 (2009). DOI: <https://doi.org/10.1016/j.conbuildmat.2007.12.011>
- [13] J. Duszczyk; K.vSiuzdak, T. Klimczuk, J. Strychalska-Nowak, A. Zaleska-Medynska, Modified Manganese Phosphate Conversion Coating on Low-Carbon Steel. *Materials; Basel.* **13**, 6, 1416 (2020). DOI: <https://doi.org/10.3390/ma13061416>
- [14] Y. Xiaohua, W. Ruwei, Y. Laishun, Preparation of Zinc-manganese Phosphating Coating on Q235 Steel and Its Environmental-friendly Sealing Treatment. *Int. J. Electrochem. Sci.* **17**, (2022), Article Number: 220548. DOI: <https://doi.org/10.20964/2022.05.43>
- [15] N. Trong-Linh, C. Tsung-Chieh, C. Jung-Yen, P. Chun-Jern, L. Tzu-Hsiang, A zinc–manganese composite phosphate conversion coating for corrosion protection of AZ91D alloy: growth and characteristics. *Journal of Materials Research and Technology* **19**, 2965-2980 (2022). DOI: <https://doi.org/10.1016/j.jmrt.2022.06.079>
- [16] A. Heydarian, A. Abolhassan Najafi, G. Khalaj, Enhancement of low-zinc phosphate coatings with addition Ni<sup>2+</sup> and Mn<sup>2+</sup> cations: Structure, corrosion resistance and paint adhesion. *J. of Materials Research and Technology* **30**, 7308-7327 (2024).